Earth Surface Processes and Landforms
Earth Surf. Process. Landforms **24**, 641–652 (1999)

MODELLING ALLUVIAL FAN MORPHOLOGY

LAWRENCE J. DE CHANT[1], PATRICK P. PEASE[2]* AND VATCHE P. TCHAKERIAN[3]
[1]*Mail Stop D413, Los Alamos National Laboratory, Los Alamos, NM 87545, USA*
[2]*Department of Geography, East Carolina University, Greenville, NC 27858-4353 USA*
[3]*Departments of Geography and Geology & Geophysics, Texas A & M University, College Station, TX 77843, USA*

Received 23 June 1997; Revised 5 November 1998; Accepted 17 November 1998

ABSTRACT

A mathematical model which estimates the scale-independent sediment surface profile of alluvial fans has been developed. This model utilizes a diffusive sediment transport model and an unsteady, radial flow, conservation relationship. These equations are approximately solved assuming a quasi-steady-state closure with appropriate modelling assumptions for two end member fan types: (1) fans where most of the fan surface is depositionally active (denoted here as 'homogeneous') and (2) fans characterized by channelling and sediment sorting processes. The fundamental result for these two fan types is a dimensionless sediment profile relationship which approximates most fan surfaces. The model suggests that the overall dimensionless morphology of alluvial fans is governed more by fundamental diffusion principles in sediment deposition than by individual environmental or basin characteristics. Additionally, this work potentially can be extended to model temporal variation in fan development. Preliminary comparison with alluvial fan profiles is reasonable, indicating that this model provides useful qualitative and quantitative information relating to alluvial fan process and morphology. Copyright © 1999 John Wiley & Sons, Ltd.

KEY WORDS: Alluvial fans; modelling; fan hydrology; fan sedimentology

INTRODUCTION

Alluvial fans are sedimentary deposits formed at the base of mountain fronts as they emerge onto valley floors. They consist of grain sizes ranging form boulders to silt and clay. The plan-form morphology of an alluvial fan is roughly triangular, whereas the three-dimensional morphology more closely resembles a cone segment. The cone apex rests at the point where the stream issues from a steep channel onto a valley floor at which point the flow becomes unrestricted (*cf.* Blair and McPherson, 1994a; Bull, 1977). Fans typically range in size from 0·5 to 10 km in length and develop from the deposition of sediment at the slope transition between the upland stream and a valley floor, where the stream loses competence (Blair and McPherson, 1994a). The flow spreads outward in a radiating pattern from the fan head. This results in the thinning of sediments toward the distal reaches of the fan (Bull, 1977), and in some instances the deposition pattern leads to a proximal distance sorting of sediment size (Miall, 1996). Figure 1 provides a schematic representation of an alluvial fan system with nomenclature appropriate for this work and Figure 2 shows a photograph of a typical fan system.

A number of factors have been suggested to explain fan morphology, including tectonic setting, climate, topography and lithology (Lecce, 1990, 1991; Bull, 1977). Some of the most common relations are size of basin area to fan size (Blair and McPherson, 1994a), feeder channel slope to fan slope (Blair and McPherson, 1994a), and basin lithology to fan size (Lecce, 1991).

Processes associated with alluvial fan systems are important for several reasons. Modern alluvial fan environments are potentially high-risk regions for human habitation and development. Phoenix, Salt Lake City and Las Vegas have all experienced major floods associated with alluvial fans (French, 1987).

* Correspondence to: Dr P. Pease, Department of Geography, East Carolina University, Greenville, NC 27858-4353, USA. Email: PeaseP@mail.ecu.edu

CCC 0197-9337/99/070641–12 $17.50

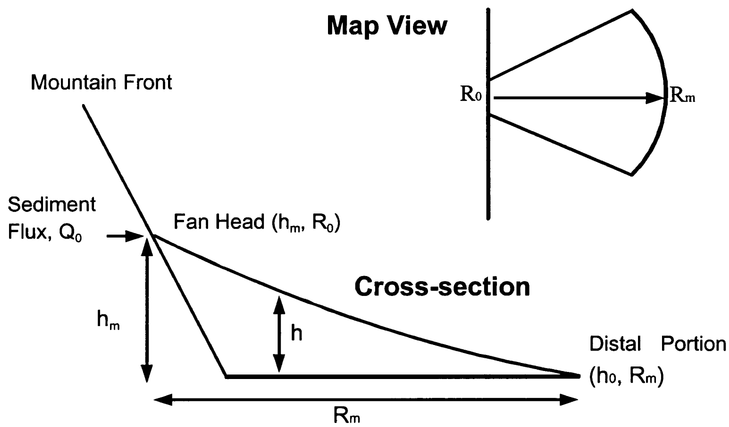

Figure 1. Simple schematic diagram of alluvial fan morphology with terminology used in this paper.

Figure 2. Photograph of alluvial fans emerging from the Panamint Mountains, Death Valley, California. The large fan on the right is Trail Canyon Fan which is included in this study. Note the channel development on the fans

Additionally, alluvial fans and desert fluvial systems provide important modern and ancient reservoirs for water and petroleum. Alluvial fans are also important indicators of tectonic, neotectonic and palaeoclimatic activity (Bull, 1977; Rust and Koster, 1984).

Modelling of alluvial fan deposition on a geological time scale, as well as on an engineering time scale, is discussed in detail by French (1987). Price (1972) developed a 'random walk' model discussed also by Rachoki (1981) and Scheidegger (1961). Using a stochastic formulation, these models describe the formation and spreading of braided channels and bars across the fan surface. The variables in the 'random walk' model of Price (1972) include tectonics, fluvial and debris transport processes. Tetzlaff (1992) developed another model applicable to an alluvial fan example. The model by Tetzlaff (1992) is deterministic, but retains a random character because of the non-linearity of the governing equations. French (1992a, b) developed a set of stochastically based models to quantify spatial and temporal risks associated with flood control facilities in areas dominated by alluvial fans.

The above models represent sophisticated simulation tools. Unfortunately, their complexity prevents them from routine use for simulation purposes owing to data input requirements and computational limitations and, as such, there may be considerable difficulty in discerning basic physical processes from them. This study provides an alternative to these models and proposes a reduced mathematical model that can provide basic information concerning fan deposition. For a large population of events, a close connection may be drawn between a random walk process (*cf.* Price, 1972) and a simple diffusive process which is implemented here. This connection has been exploited in the field of high temperature gas dynamics and kinetic theory to analytically predict transport phenomena (Anderson, 1989). No attempt is made to formally relate the gradient transport model developed later to a stochastic analysis beyond the analogy drawn with gas dynamics or the intuitive concept of a large number of local fan channels being 'averaged/smeared' into a single transport equation.

Though we will discuss boundary conditions and their implementation subsequently, it is worth noting that it is our desire to obtain a model that can be successfully used with a minimum of empirically measured parameters. Examples of parameters that would be very expensive to measure or could be completely unattainable might include, Q_0, the average sediment influx rate, in say cubic metres per year. The current formulation bypasses the necessity for information of this type, by non-dimensionalizing. In summary, the model provides a 'snap shot' of alluvial fan morphology. It is not the goal of this work to provide a time-dependent parameter requirement demanding dynamic sediment deposition model (e.g. Tetzlaff, 1992). This type of simulation, while interesting, cannot be used to compare a wide variety of fan morphologies, since detailed parameters are usually not available.

THEORETICAL MODEL

A simple mathematical model which approximately describes the morphology of alluvial fans is presented. Analysis of an alluvial fan begins by considering the mass conservation statement: [Time rate of change of sediment within the control volume] = [Flux of sediment entering] − [Flux of sediment leaving].

Mathematically, this relationship with reference to Figure 1 yields:

$$\frac{\partial}{\partial t}[hr\mathrm{d}r\mathrm{d}\theta] = [qbr\mathrm{d}\theta] - \left[(q + \frac{\partial q}{\partial r}\mathrm{d}r)(r + \mathrm{d}r)b\mathrm{d}\theta\right] \tag{1}$$

where h is the fan height above a datum (the valley floor on which the fan is developed), r is the fan radius, b is the sediment flow depth and q is the average sediment velocity. Simplifying Equation 1 provides the time-dependent, 1 − d, axisymmetric, mass conservation equation:

$$\frac{\partial h}{\partial t} = -\frac{1}{r}\frac{\partial}{\partial r}(brq) \tag{2}$$

Equation 2 assumes constant sediment density and incompressibility. Closure to this equation requires a model for the sediment velocity or, equivalently, the sediment flux. Following Kirkby (1980) and Dunne and Aubry (1986) an analogous model is proposed of the form:

$$q \propto -(\nu_{\mathrm{hyd}})(slope) \tag{3}$$

The local hydraulic velocity (V_{hyd}) in Equation 3 introduces a new unknown. The local hydraulic velocity, though, by invoking a steady source flow continuity relationship, i.e. $Q_{\mathrm{hyd}} \propto v_{\mathrm{hyd}}A \propto v_{\mathrm{hyd}}r = v_{\mathrm{hm}}R_{\mathrm{m}}$ (Q = discharge, A = area, R_{m} = maximum fan radius, V_{hm} = maximum velocity). The subscript 'hyd' is retained to emphasize that these are the average fluvial velocities. We note that this simple control volume approximation has neglected the effect of percolation and evaporation. Clearly, a more detailed model could include these effects, yielding a modified and more complexly spatial dependent hydraulic velocity, v_{hyd}. In our experience, however, there is more to be gained by using the least complex sediment velocity closure, rather than attempting to retain these effects. Algebraically rearranging:

$$\nu_{\text{hyd}} \equiv \nu_{\text{hydm}} \frac{R_{\text{m}}}{r} \tag{4}$$

and substituting into Equation 3, yields:

$$q = -(const.)\nu_{\text{hydm}} \frac{R_{\text{m}}}{r} \frac{\partial h}{\partial r} \equiv -K \frac{R_{\text{m}}}{r} \frac{\partial h}{\partial r} \tag{5}$$

where $-k$ is sediment velocity (L/t).

Substituting Equation 5 into Equation 2 provides the governing relationship:

$$\frac{\partial h}{\partial t} = \frac{kbR_{\text{m}}}{r} \frac{\partial}{\partial r}\left(\frac{\partial h}{\partial r}\right) \tag{6}$$

Equation 6 takes the form of an unsteady heat equation. A similar governing equation has been used by Paola *et al.* (1992) to study large-scale depositional basin characteristics. Boundary and initial conditions for this partial differential equation are required. The first condition requires that the sediment flux at the fan head be specified and constant. Sediment flux is not constant on an engineering time scale. However, we are interested in long-term development and when sediment flux is considered in geological time, short-term (seasonal scale, or even annual) fluctuations can be averaged by a continuum or constant sediment influx, Q_0. This average process would take the form of:

$$Q_0 \equiv \frac{1}{T} \int_0^T Q_{\text{seasonal}}(t)\text{d}t \tag{7}$$

Equation 7 performs a seasonal temporal averaging. Clearly, however, if we consider the sediment flux to be absolutely constant, temporal changes on the geological scale, such as change in catchment area, basin denudation, tectonic modifications of total relief, have been lost as well. The necessity for this limitation is due to the desire to obtain a model which can be successfully used with a minimum of empirically measured parameters. It is not the goal of this work to provide a time-dependent parameter requiring dynamic sediment deposition in the model. With this approximation, the fan head, $r = R_0$, sediment flux is specified:

$$brq\big|_{r=R_0} = -kR_{\text{m}}b\frac{\partial h}{\partial r} = Q_0 \tag{8}$$

Additionally, sediment flux at the distal portion of the fan must be estimated. As a starting approximation, it is assumed that all of the material entering the fan is deposited within the fan. An alternative way to view this approximation is to consider the sediment influx, Q_0, to be a *net*flux, i.e. $Q_0 = Q_{\text{in}} - Q_{\text{out}}$ of particles of any size. With this generalization, one could actually obtain an *eroding* fan where $Q_0 < 0$, with subsequent concave-down profile. This approximation also assumes that the majority of the sediment considered by this analysis is sand size or larger. Silt and clay sized sediment is permitted to escape the fan model. Mathematically representing the distal, $r = R_{\text{m}}$, fan behaviour:

$$\frac{\partial h}{\partial r} = 0 \tag{9}$$

Equation 9 follows from equation 5 and merely implies that at the edge of the fan, i.e. $r = R_{\text{m}}$, no sediment crosses the 'boundary' of the fan. We consider the fan to be accreting on an infinite plain. An alternative and interesting problem concerns the basin-scale problem and has been treated by Paola *et al.* (1992). Finally, by definition, at the fan toe $r = R_m$, fan height $h(r = R_m) = 0$. As the analysis is extended to take into account variable deposition and erosion on the fan, i.e. channelled versus fully homogeneous sheetflow, this assumption will be relaxed.

Since this analysis is intended to provide scale-independent information, initial conditions can be essentially ignored. This concept implies a state approaching, but not reaching, dynamic equilibrium. Dynamic equilibrium with respect to the sediment budget would imply a perfect balance between sediment inflow and outflow fluxes. In the case of a fully static or equilibrium situation the temporal term in Equation 6 approaches zero, which would result in a completely linear fan profile.

Equations 6–9 provide the basis for the following analysis. To allow for ready comparison of fans of differing sizes, Equations 6–9 can be re-expressed by rewriting into a non-dimensionalizing form and translating the r coordinate: $r - R_0 = (R_m - R_0)r^*$ and rescaling h and t: $h = (Q_0 h^*/kb)$, $t = (R_m\text{-}R_0)^2 t^*/kb$ (the superscript asterisk denotes dimensionless variables). The approximate solution of Equations 6–9 is performed by multiplying both sides by r, rewriting in terms of the dimensionless variables, and integrating Equation 6 between $r^* = 0$ and $r^* = 1$:

$$\int_0^1 \left[(1 - \frac{R_0}{R_m})r^* + \frac{R_0}{R_m}\right] \frac{\partial h^*}{\partial t^*} dr^* = \int_0^1 \frac{\partial}{\partial r}\left(\frac{\partial h}{\partial r}\right) dr^* = 0 - \frac{\partial h^*}{\partial r^*}\Big|_{r^*=0} \tag{10}$$

Introducing the non-dimensional form of Equation 7 into the right-hand side of Equation 10:

$$\int_0^1 \left[(1 - \frac{R_0}{R_m})r^* + \frac{R_0}{R_m}\right] \frac{\partial h^*}{\partial t^*} dr^* = 1 - \frac{R_0}{R_m} \tag{11}$$

Since $R_0/R_m \ll 1$, this term is neglected on both sides of Equation 11, yielding:

$$\int_0^1 r^* \frac{\partial h^*}{\partial t^*} dr^* \approx 1 \tag{12}$$

Effectively, the analysis has been reduced to a two-dimensional problem along any radial coordinate. Finally, for a homogeneous fan, a 'lumped capacitance' approach from heat transfer theory (Incropera and De Witt, 1981) or pseudo-steady-state approximation from petroleum reservoir simulation (Dietz, 1965) may be adopted. With these approximations, Equation 12 becomes:

$$r^* \frac{\partial h^*}{\partial t^*} \approx 1 \tag{13}$$

Back-substitution into Equation 6, which has also been non-dimensionalized and simplified for $R_0/R_m \ll 1$, yields the ordinary differential equation:

$$1 = \frac{d^2 h^*}{dr^{*2}} \tag{14}$$

This is the basic approximate equation defining a homogeneous (fully active) alluvial fan system. Transformed boundary conditions include $dh^*/dr^* = -1$ at $r^* = 0$ and $h^* = 0$ at $r^* = 1$. The approximations in Equation 13 need to be modified to model a channelled fan since the sediment is not equally distributed across the fan. For virtually any fan sediment, distribution as a function of clast size is not homogeneous. In this situation the lumped capacitance model is rather poor. An extension to this model is to include limited profile information in the averaging approximation:

$$\int_0^1 r^* \frac{\partial h^*}{\partial t^*} \mathrm{d}r^* \approx (1 - r^*) \frac{\partial h^*}{\partial t^*} \approx (1 - r^*) = \frac{\mathrm{d}^2 h^*}{\mathrm{d}r^{*2}} \tag{15}$$

The simple linear function used to extend the model was selected by merely choosing a function which would satisfy the two boundary conditions ($\mathrm{d}h^*/\mathrm{d}r^* = -1$ at $r^* = 0$ and $h^* = 0$ at $r^* = 1$). Physically, Equation 15 implies greater deposition in the headward reaches of the fan which is consistent with the model concerned with sand size and larger particles. The exiting sediment flux condition of Equation 9 is no longer applied, though this will have little effect since Equation 15 is no longer restricted to a homogeneous sediment distribution.

The solution of Equations 14 and 15 by integration and application of the non-dimensional boundary conditions yields, for a fully active, homogeneous fan, the profile:

$$h^*(r^*) = \frac{1}{2}(r^{*2} - 1) - (r^* - 1) \tag{16}$$

and:

$$h^*(r^*) = \frac{1}{2}(r^{*2} - 1) - \frac{1}{6}(r^{*3} - 1) - (r^* - 1) \tag{17}$$

for a fan with variable sediment depositional characteristics. Note that Equation 17 is merely Equation 16 with the addition of the term $1/6(r^{*3} - 1)$.

To facilitate comparison to a wide range of alluvial fans, Equations 16 and 17 are rescaled such that the sediment thickness varies from zero to one. This is done by defining the new profiles:

$$h^{**}(r^*) \equiv \frac{h^*}{h^*(0)} = (r^{*2} - 1) - 2(r^* - 1) \tag{18}$$

for a fully active, homogeneous fan and:

$$h^{**}(r^*) \equiv \frac{h^*}{h^*(0)} = \frac{3}{4}(r^{*2} - 1)) - \frac{1}{4}(r^{*3} - 1) - \frac{6}{4}(r^* - 1) \tag{19}$$

for a fan with variable sediment depositional characteristics.

In summary, an approximate model for scale-independent fan deposition using mass conservation considerations and a diffusive sediment transport model is developed. The resulting partial differential equation is simplified and integrated to yield a set of dimensionless fan profiles. These two profiles are intended to model, at least as end members, fully active fans and locally channelized fans.

The macroscopic processes of slope decay, fan deposition, stream profile gradient, etc. are composed of a large number of complex events covering a wide range of time and space scales. For example, a single flood event is composed of innumerable rotations and movements of individual grains or particles. Small rills and channels, move, deposit, erode and redeposit in a highly complex, essentially stochastic manner. There is a close analogy between these complex micro-events and modelling of the vibration of individual atoms in a solid at an elevated temperature.

Since we have little hope of capturing the process of every small event, it might make sense to define an empirical law in terms of macroscopic quantities, i.e. local fan slope or temperature gradient. Fourier's law of heat transfer reaffirms our macroscopic notion that heat flows from a hot solid body to a cold environment. A similar analogy is that sediment flows from regions of high relief and deposits in areas of low local relief. We

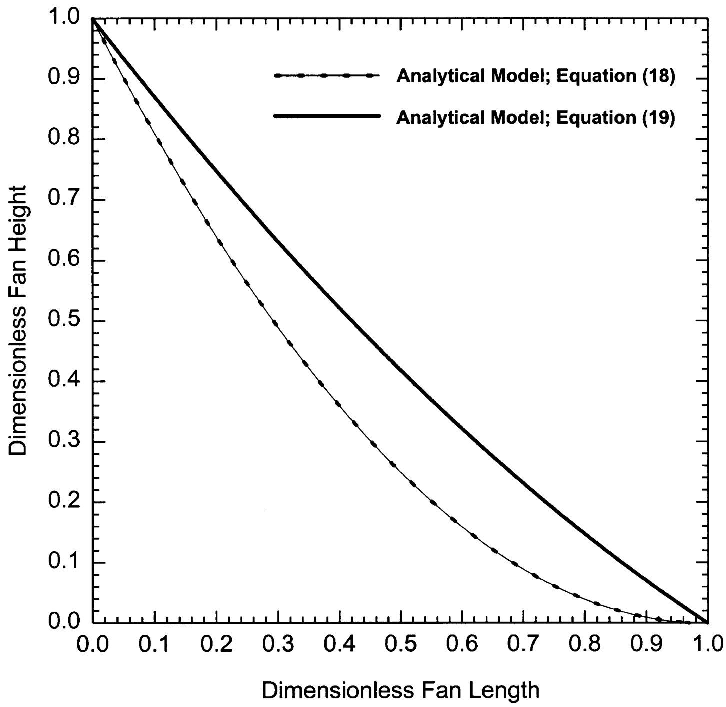

Figure 3. Comparison of analytical models derived for homogeneous sheetflow fan deposition (Equation 18) and channelled fan deposition (Equation 19).

have taken the enormous complexity of that process and said that, on average, this sediment movement will occur. In the next section, measurements from 20 fans are compared to Equations 18 and 19.

COMPARISON OF MODEL AND DATA

Because of wide variations in fan sizes and factors which contribute to their development, testing of the validity of any morphological model, in this case Equations 18 and 19, should be viewed as a first approximation. With the latter constraint in mind, the models developed in this study are compared to topographical measurements of 20 fans.

Figure 3 shows the relation between the models presented in Equations 18 and 19 and measured dimensionless fan morphologies for 20 alluvial fans. The fans were selected to represent a variety of fan sizes and settings. The individual fan locations are presented in Table I. Data were taken from 7·5 minute US Geological Survey topographic maps along three different radial transects for each fan. Between 12 and 70 individual data points were extracted from each fan, depending upon the size of the fan. Figure 4 indicates that, overall, the comparison of the fans to the simple models developed here is reasonable. The data cluster well around Equation 19, indicating that fan morphology is clearly described by the channelized flow model. Equation 18 does not explain any of the fan data, but has been included since it emphasizes the importance of adequately modelling inflow and outflow sediment budgets and problems associated with assuming sustained homogeneous sheetflow on fans.

Table I. Alluvial fans used for data collection and their location

Alluvial fan name	Map quadrangle name	State
Marble Canyon	East of Sands Flat	California
Trail Canyon	Devils Speedway	California
(Unnamed)	Dry Bone Canyon	California
Niter Beds	East of Sands Flat	California
Surprise Canyon	Ballarat	California
(Unnamed)	Stewart Valley	California – Nevada
(Unnamed)	Death Valley Junction	California
Mosaic Canyon	Stovepipe Wells	California
Cave Canyon	Cave Canyon	Utah
Fishers Wash	Lund	Utah
Icehouse Canyon	Rhyolite Ridge SW	Nevada
Trough Spring	Sunnyside	Nevada
Little Dog Canyon	Gowdy Ranch	New Mexico
Indian Draw	Indian Draw	New Mexico
Bear Canyon	Lake Lucero	New Mexico
Sulpher Canyon	Black Top Mountain	New Mexico
Alamo Canyon	Alamogordo South	New Mexico
Telephone Canyon	Stillwell Crossing	Texas
Cedar Creek	Ennis	Montana
Indian Butte	Antelope Peak	Arizona

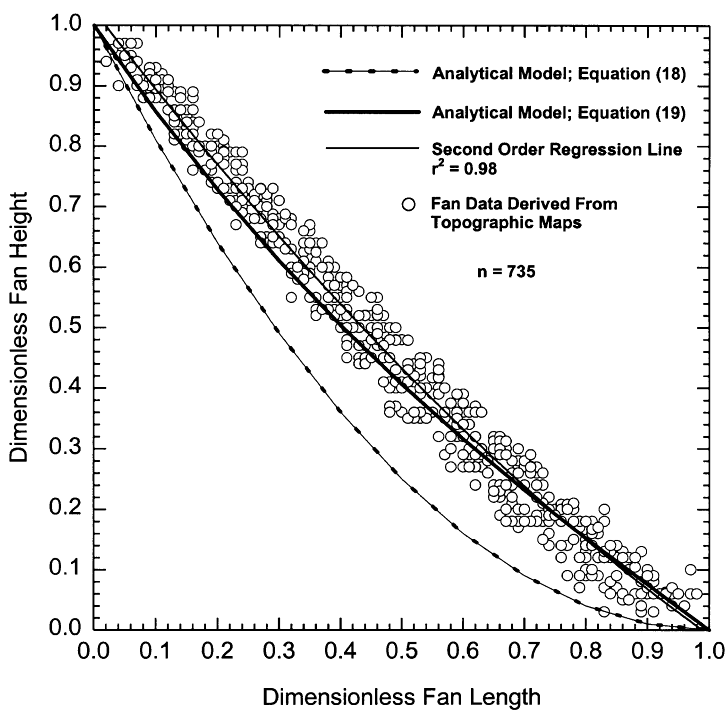

Figure 4. Comparison of the two models for fan profiles derived in this paper (Equations 18 and 19) with data from 20 alluvial fans. Data are shown in dimensionless form to facilitate comparisons between fans of different sizes. The second order regression line is included to show the fit of the model for Equation 19 with the fan data points

Deviations in local curvature (keeping in mind that the measurements and the model are dimensionless, hence the exact fit at the end points is not an independent verification, whereas the curvature is) between fan data and the model are probably the result of a number of variables, including local anomalous variation in fan morphology, vegetation cover, scale problems associated with data extraction from topographic maps, and the simplifications in the current model. As shown in Figure 4, there is a slight underestimation of the

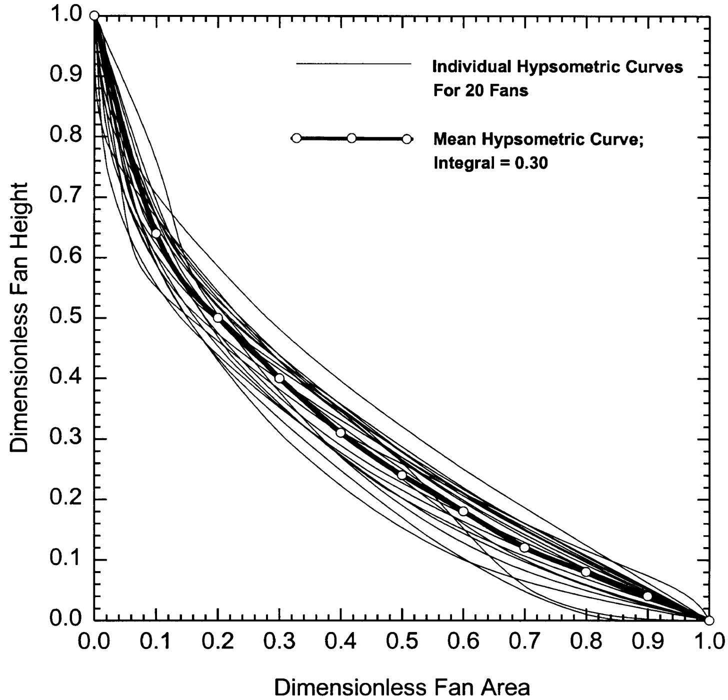

Figure 5. Hypsometric curves for the 20 alluvial fans examined in this paper, and the mean curve for the 20 individual curves. The mean hypsometric integral (volume of the fan relative to a reference volume of 1·0) derived from the mean curve is 0·30

model in the upper, proximal fan area. Since the model assumes a diffusion distribution of mass it may not account for the possibility of an anomalously large mass, such as mass movement delivered boulders, not directly related to flow which might be deposited preferentially near the fan head. Miall (1996) pointed out that such a size distribution is often present in fan facies, and Blair and McPherson (1994a) noted that the slope steepness increases with increasing grain size. Such steepened slopes (unrelated to flow mechanisms) in the proximal region may be responsible for the model's underestimation in that area. With these variables and simplifications in mind, Equation 19 has a favourable fit as seen in Figure 4. The mathematical simplicity of this model is not a detriment, and would be particularly useful to geoscientists, given the often limited data available for the morphologic examination of modern and ancient alluvial systems.

With access to the dimensionless profile Equation 19, it is possible to further describe alluvial fan morphology in terms of a single parameter, i.e. a hypsometric integral. A hypsometric integral scales a landform volume to non-dimensional space, allowing the direct comparison of a variety of examples (*cf.* Strahler, 1952). This involves scaling the fan volume by a reference volume. For an alluvial fan, the reference volume is the smallest cylinder slice (pie wedge) that the fan can fully fit within. Considering first a two-dimensional profile, the normalized hypsometric integral is:

$$\Gamma_{2-\mathrm{d}} = \frac{V_{2-\mathrm{d,actual}}}{V_{2-\mathrm{d,possible}}} = \frac{\int_0^1 h^{**}(r^*)\mathrm{d}r^*}{(1)(1)} \tag{20}$$

where $h^{**}(r^*)$ is either equation 18 or 19. For the better fitting cubic Equation 19, $\Gamma_{2\text{-d}} = 7/16 \cong 0{\cdot}44$. Hypsometric curves for the 20 fans used in this study are shown in Figure 5. The hypsometric data represent the three-dimensional volume of fans (L^3) whereas the model Equation 19 is the two-dimensional fan profile.

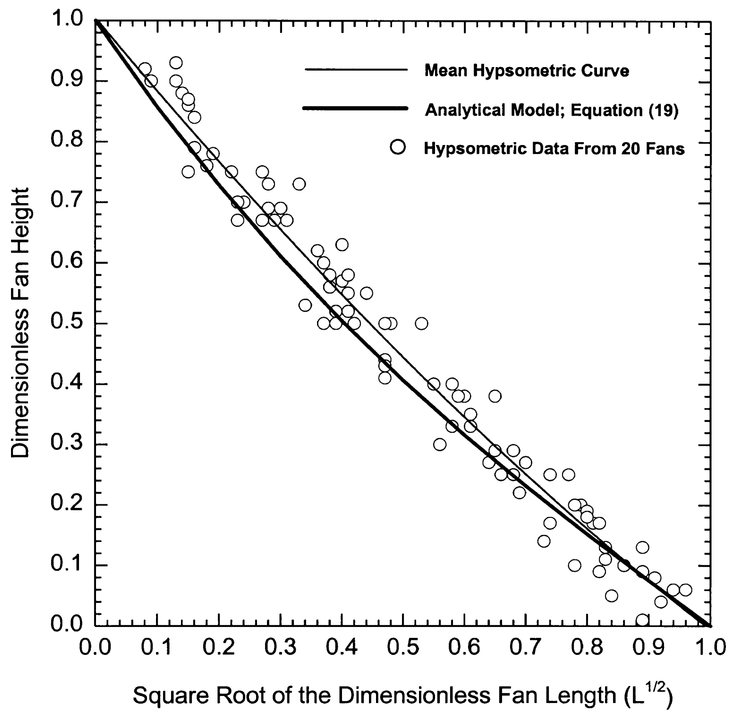

Figure 6. Comparison of Equation 19 with redimensionalized hypsometric data from 20 alluvial fans. The hypsometric data are redimensionalized so that they can be directly compared with Equation 19. Circles represent data points to which the mean hypsometric curve is fitted.

The two are very similar with the two-dimensional model integral of 0·44 and the two-dimensional mean fan integral of 0·46. The non-dimensional space in which the fan profile is plotted does not account for the third, width dimension of a fan and, thus, represents only 2/3 of the total reference volume. Therefore, 0·44 represents the hypsometric integral of 66 per cent of the reference volume. To compare the two, the data in Figure 5 are redimensionalized in Figure 6 by plotting the height percentage of fans against the square root of the percentage area. This redimensionalization enables the data to be compared with equation 19. Figure 6 shows the close fit of Equation 19 with the fan hypsometric data, and the mean hypsometric curve for the 20 fans.

Since a two-dimensional integral does not provide a directly meaningful value for the volume of an alluvial fan, a three-dimensional 'sector of a cone' integral is applied. This three-dimensional integral takes the form:

$$\Gamma_{3-\mathrm{d}} = \frac{V_{3-\mathrm{d,actual}}}{V_{3-\mathrm{d,possible}}} = \frac{\int_0^1 h^{**}(r^*) r^* \mathrm{d}r^*}{\int_0^1 r^* \mathrm{d}r^*} \tag{21}$$

The associated hypsometric integral $\Gamma_{3\text{-d}} = 11/40 \cong 0{\cdot}28$. This value is nearly identical to the mean hypsometric integral of 0·30 for the 20 fans listed in Table I and shown in Figure 5. The variation can be attributed to the slight underestimation of the model as compared to actual data. This indicates that not only are the dimensionless profiles of alluvial fans uniform, but so is their distribution of mass.

This implies that the diffusion of sediment occurs at the same rate irrespective of the surrounding environment. In other words, sediment diffusion and deposition occur at the same rate for unconfined fans with nearly 180° arcs as in confined fans with narrowed arc lengths, given the profile uniformity of fans as a limiting factor on mass distribution.

Since the dimensionless fan profiles and hypsometric distribution of most fans can be described based on Equation 19, overall fan morphology and volume can also be represented. A practical application of the integration value given in Equation 21 is the direct comparison of the value to dimensional reference volumes. As stated above, the reference volume is the cylinder wedge in which the fan can be enclosed. Using the hypsometric integral of 0·28 from Equation 21 (based on Equation 19), the volume of an alluvial fan can be estimated with the equation:

$$V \cong 0 \cdot 28\left(\frac{\theta}{360}\pi r^2 h\right) \tag{22}$$

where V is fan volume, θ is the mean angle of the fan wedge, and r and h are the maximum fan radius and total height at the fan head, respectively (in desired units). Equation 22 will yield fan volumes above fan toe datum. It should be noted that only volume above the datum is estimated and this model does not account for basin subsidence.

Although this work treated alluvial fans as if they are in a steady-state condition, clearly they are not. Irrespective of environmental variables, a fan system will grow in size with the addition of sediment. A discussion of this growth is summarized below. Referring to Equation 12, a relationship may be written:

$$\left(\frac{R_{\mathrm{m}}}{R_0}\right)^2 \frac{\mathrm{d}}{\mathrm{d}t^*}\left(\frac{R_{\mathrm{m}}}{R_0}\right) \approx 1 \tag{23}$$

which is solved to yield:

$$\frac{R_{\mathrm{m}}}{R_0} \propto t^{*\frac{1}{3}} \tag{24}$$

The 1/3 power growth of the fan radius, rather than 1/2 power which might be expected from dimensional grounds for a radial flow problem (Freeze and Cherry, 1979) is related to the closure chosen for the sediment flux (Equation 5). Further work will be needed to develop the unsteady analysis further. Additionally, the approximations applied here might be relaxed and the full partial differential equation solved by similarity methods. Finally, the encouraging results from this study indicate that the very complex processes associated with intermittent fluvial processes can potentially be modelled using approximate, analytical methods.

CONCLUSIONS AND RECOMMENDATIONS

An elementary mathematical model which estimates the scale-independent sediment elevation profile of an alluvial fan has been developed. The model, which is derived using a diffusive sediment transport model and an unsteady, radial flow, conservation relationship, yields a dimensionless relationship describing fan sediment thickness. Two different solutions are obtained which model end member fan types: (1) 'homogeneous' fans where most of the fan surface is depositionally active, and (2) fans characterized by well defined channelling processes. Data clearly show that the model defining channelled processes provides the best fit for all fans examined in this study. This might result from the improbability of developing fans in which the entire surface is uniformly active. The model also suggests that environmental variables (e.g. climate, lithology) play a less significant role in overall fan morphology than do basic sedimentary and flow processes. External factors are still important, since they contribute to fan initiation, total sediment supply and overall fan size. However, the uniformity of the sedimentary geometry of fans suggests a more ubiquitous process responsible for fan morphology: that of basic diffusion principles. Additionally, this work can potentially be extended to model temporal variation in the growth of fans. The analytical solutions obtained here are shown to be consistent with previous, empirically obtained relations. The results of the channelled model (Equation 19) show a good comparison with profiles from a 20 fan data set. As such, this elementary model can provide useful qualitative and quantitative information relating to alluvial fan process and morphology. This is of direct interest for modern alluvial fan systems, as well as for identifying and understanding ancient fluvial environments.

REFERENCES

Anderson, J. D. 1989. Hyposonic and High Temperature Gas Dynamics, McGraw-Hill, New York.

Blair, T. C. and McPherson, J. G. 1994a. 'Alluvial fan processes and forms', in Abrahams, A. D. and Parsons, A. J. (Eds), Geomorphology of Desert Environments, Chapman and Hall, London, 354–402.

Blair, T. C. and McPherson, J. G. 1994b. 'Alluvial fans and their natural distinction from rivers based on morphology, hydraulic processes, sedimentary processes, and facies assemblages', *Journal of Sedimentary Research*, **A64**, 450–489.

Bull, W. B. 1964a. Geomorphology of Segmented Alluvial Fans in Western Fresno County California, USGS Professional Paper, **352-E**.

Bull, W. B. 1964b. Alluvial Fans and Near-Surface Subsidence in Western Fresno County California, USGS Professional Paper, **282-F**.

Bull, W. B. 1977. 'The alluvial-fan environment', *Progress in Physical Geography*, **1**, 222–270.

Chorley, J. C. and Schumm, S. A., Sugden, D. E. 1984. Geomorphology, University Press.

Conybeare, C. E. 1976. Geomorphology of Oil and Gas Fields in Sandstone Bodies, Elsevier, Amsterdam.

Dietz, D. N. 1965. 'Determination of average reservoir pressure from buildup surveys,' *Journal of Petroleum Technology*, August, 955–959.

Dunne, T. and Aubry, B. F. 1986. in Abrahams, A. D. (Ed.), Hillslope Processes, Allen & Unwin.

Freeze, R. A. and Cherry, J. A. 1979. Groundwater, Prentice-Hall.

French, R. H. 1987. Hydraulic Processes on Alluvial Fans, Elsevier, Amsterdam.

French, R. H. 1992a. 'Alluvial fans,' *Journal of Hydraulic Engineering*, **118** (7) 1002–1013.

French, R. H. 1992b. 'Design of flood protection for transportation alignments on alluvial fans,' *Journal of Irrigation and Drainage Engineering*, **118** (2), 320–330.

Hunt, C. B. and Mabey, D. R. 1966. Stratigraphy and Structure, Death Valley, California, US Geological Survey Professional Paper **494-A**.

Incropera, F. P. and De Witt, D. P. 1981. Fundamentals of Heat and Mass Transfer, Wiley.

Kirkby, M. J. 1980 'Modeling water erosion processes,' in Kirkby, M. J. and Morgan, R. P. C. (Eds) Soil Erosion, Wiley, 183–216.

Lecce, S. A. 1990. 'The alluvial fan problem', in Rachocki, A. H. and Church, M. (Eds), Alluvial Fans: A Field Approach, John Wiley, Chichester, 3–24.

Lecce, S. A. 1991. 'Influence of lithologic erodibility on alluvial fans area, Western White Mountains, California and Nevada', *Earth Surface Processes and Landforms*, **16**, 11–18.

Miall, A. D. 1996. The Geology of Fluvial Deposits, Springer, Berlin.

Paola, C. and Heller, P. L., Angeuine, C. L. 1992. 'The large-scale dynamics of grain size variation in alluvial basins 1, Theory,' *Basin Research*, **4**, 73–90.

Price, W. E. 1972. 'Simulation of alluvial fan deposition by a random walk model,' *Water Resources Research*, **10**(2), 263–274.

Rachocki, A. 1981. Alluvial Fans, Wiley.

Rust, B. R. and Koster, E. H. 1984. in Walker, R. G. (Ed.) Facies Models, 2nd edn Geoscience Canada.

Scheideggar, A. E. 1961. Theoretical Geomorphology, Prentice-Hall, Englewood Cliffs.

Stone, R. O. 1967. 'A desert glossary,' *Earth Science Reviews*, **3**, 211–268.

Strahler, A. N. 1952. 'Hypsometric (area– altitude) analysis of erosional topography', *Geological Society of America Bulletin*, **63**, 1117–1142.

Tetzlaff, D. M. 1992. 'Predictive computer simulation of clastic sedimentary processes,' in Fitzgibbon, W. E. and Wheeler, M. F. (Eds), Modeling and Analysis of Diffusive and Advective Processes in Geosciences, Society of Industrial and Applied Mathematics, 205–221.

